Available online at www.sciencedirect.com
ScienceDirect
Journal of Magnetic Resonance 190 (2008) 86–94
JMR Journal of Magnetic Resonance
www.elsevier.com/locate/jmr

Auxiliary phase encoding in multi spin-echo sequences: Application to rapid current density imaging

Igor Serša *

Jožef Stefan Institute, Jamova 39, 1000 Ljubljana, Slovenia

Received 13 June 2007; revised 15 October 2007
Available online 23 October 2007

Abstract

Multi spin-echo sequences such as single-shot RARE are very sensitive to the initial phase of the transverse magnetization, and they can preserve only the transverse magnetization component which is aligned with the axis of the refocusing pulse rotation. Therefore, two separate single-shot RARE experiments with phases of refocusing pulses 90° apart have to be run and their complex images summed to obtain an error-free phase map of the initial transverse magnetization. This is particularly useful when auxiliary phase encoding is integrated in the preparation period of the RARE sequence, such as when encoding flow, displacement, susceptibility, pH or temperature. In this paper, the two-shot RARE approach is verified first theoretically and then experimentally by demonstrating its application to rapid current density imaging (CDI). The sequence consists of the preparation period which triggers electric pulses in the sample followed by the RARE acquisition period. Electric currents through the sample induce a magnetic field change in the direction of the static magnetic field and a phase change of the initial magnetization proportional to it. To calculate one component of current density two orthogonal components of magnetic field change must be measured. In general, for 2D non-symmetrical samples, this can be done by rotating the sample to a perpendicular orientation. The proposed CDI method allows much for faster magnetic field change mapping than the standard spin-echo based CDI.

Keywords: Spin-echo; Sequence stability; Auxiliary phase encoding; Fast MR imaging; Current density imaging

1. Introduction

Multi spin-echo (MSE) sequences are very sensitive to the flip angle of refocusing pulses in the RF pulse train. Any deviation from the ideal 180° flip angle leads to a complete loss of the transverse magnetization component in the direction perpendicular to the axis of rotation of the refocusing pulses, i.e., the non-Meiboom–Gill (MG) component. For this reason the simple Carr–Purcell (CP) sequence [1] ($\pi/2[x] - (\tau - \pi[x] - \tau)^N - \mathrm{AQ}$), in which the phases of all RF pulses are identical, loses practically all transverse magnetization after only a few echoes. However, its MG modification (CPMG) [2] ($\pi/2[x] - (\tau - \pi[y] - \tau)^N - \mathrm{AQ}$), in which refocusing pulses are shifted by 90° with respect to the phase of the excitation pulse, preserves practically all transverse magnetization. The initial transverse magnetization phase may be altered after the excitation pulse, either intentionally by auxiliary phase encoding or unintentionally by diffusion weighting, eddy currents, patient movement, or susceptibility effects. In this case neither of the two sequences will preserve the initial transverse magnetization phase and the transverse magnetization magnitude will be, in general, attenuated more than would be expected due to T_2 relaxation. For this reason the standard MSE imaging sequence, i.e., the RARE sequence [3], has image artefacts in the form of signal voids in regions with non-MG initial transverse magnetization.

A simple but not entirely satisfactory solution to this problem was first offered by Maudsley [4] who suggested the use of alternate x and y phases of refocusing pulses. Better results can be obtained by some more sophisticated

* Fax: +386 1 477 3191.
E-mail address: igor.sersa@ijs.si

1090-7807/$ - see front matter © 2007 Elsevier Inc. All rights reserved.
doi:10.1016/j.jmr.2007.10.009

phase schemes that were suggested by Guillon et al. [5]. In these schemes, refocusing pulses are followed by lists of interchanging x and y or x and $-x$ phases up to 16 elements long (e.g., XY-16, MLEV-16). Both approaches aim to preserve the entire transverse magnetization and its initial phase. Based on the analysis of MSE sequences with low refocusing flip angles [6], Norris developed the ultra fast low refocusing flip angle variant of the RARE method, the U-FLARE method [7]. In addition to considerably lower deposited RF power, this method may excel in insensitivity to the initial transverse magnetization phase if even or odd echoes are removed from the acquisition window by the use of displaced (incoherent) U-FLARE [8]. Another approach to avoid the initial phase sensitivity problem of MSE sequences was suggested by Alsop [9]. He suggested the use of special dephasing gradients that spread the initial magnetization phases within each image voxel equally between the MG and non-MG components thus preventing signal voids due to the non-MG magnetization component being destroyed during the MSE pulse train. Alsop's approach is effective whenever preservation of the initial transverse magnetization phase is not important; for example, in diffusion weighted imaging by MSE sequences. SPLICE [10] proposed by Schick is another MSE method for fast diffusion imaging insensitive to motion artefacts. The SPLICE method uses a stimulated echo sequence for the diffusion weighting preparation. The displaced U-FLARE sequence by Norris, the dephasing gradient approach by Alsop and Schick's approach have in common the loss of one half of the transverse magnetization. Perhaps the most sophisticated MSE sequence that is insensitive to the initial transverse magnetization phase is the method proposed by Le Roux [11]. Le Roux's method, which is based on the application of quadratic phase modulation on the refocusing pulses [12], preserves the entire transverse magnetization as well as its initial phase. However, its application is quite difficult as the method requires precise adjustments of the receiver phase and the procedure for calculating the list of refocusing pulse flip angles and phases is quite complicated. This method has already been successfully applied to MR thermometry [13] in which a temperature map was obtained by mapping magnetization phase shifts caused by the precession frequency shifts induced by temperature changes in the sample.

In addition to MR thermometry there are several other methods which use auxiliary phase encoding to image various physical phenomena (flow, magnetic field susceptibility, chemical shifts, electric currents, etc.). These methods have a common preparation period in which magnetization phases are shifted, usually proportionally to the magnitude of the investigated phenomenon, but differ in their acquisition period which follows the preparation period. If acquisition is done by the MSE sequence then special care must be taken to ensure that it is insensitive to the initial transverse magnetization phase and that this phase is preserved. The standard RARE sequence preserves just the MG component of the initial transverse magnetization, which tends towards the equilibrium magnetization multiplied by the sine of half of the refocusing flip angle, and due to dispersion of off-resonance frequencies almost completely destroys the non-MG component [14]. Thus the execution of just one single-shot RARE sequence [15,16] is insufficient to acquire the initial transverse magnetization phase accumulated during the preparation period. This can be achieved by two single-shot RARE sequences that have phases of refocusing pulses 90° apart, i.e., the CP and the CPMG single-shot RARE sequence, and start at the echo following identical preparation periods. The CP and the CPMG sequences will acquire the x and y components of the initial transverse magnetization, respectively. The signals of the two single-shot RARE sequences are then summed to obtain the correct phase of the initial transverse magnetization. The sequence is therefore named the two-shot RARE sequence.

The two-shot RARE method has been applied to current density imaging (CDI) to demonstrate the use of the method and to verify experimentally its stability to the initial magnetization phase. In CDI [17,18], images of electric current density are calculated from the images of phase shifts caused by the magnetic field change due to electric current pulses flowing through the conductive sample. The proposed two-shot RARE CDI method allows much faster acquisition of the magnetic field change than the conventional CDI and is therefore appropriate for dynamic CDI experiments such as chemical reactions releasing ions [19]. A major obstacle in performing dynamic CDI is a need to rotate the sample to perpendicular orientations to acquire different magnetic field change maps needed to calculate current density images. However, there are a few sample/current arrangements where rotation is not needed and for these the proposed CDI method may be very useful in a view of dynamic CDI. One such arrangement is the cylindrical symmetry of the sample, which is presented in this paper, and the other is when currents are distributed within a thin slice [20]. In addition, the CDI technique that images radiofrequency currents (RF-CDI) [21] does not require sample rotation to obtain CD images. RF-CDI uses only a different preparation period than conventional CDI and can also be integrated into the two-shot RARE sequence. Possible application of dynamic RF-CDI is in monitoring electrical ablation therapies [22].

2. Theory

The trajectory of the magnetization vector during the MSE sequence depends on the static magnetic field inhomogeneity, imaging gradients, the initial phase, the refocusing pulse flip angle and the phases of the refocusing pulses. The spin-echo is formed in the middle of two adjacent refocusing pulses (Fig. 1a). Suppose that the magnetization vector is observed in a small volume element where the static magnetic field inhomogeneity and imaging gradients are such that the magnetization accumulates a phase shift β in

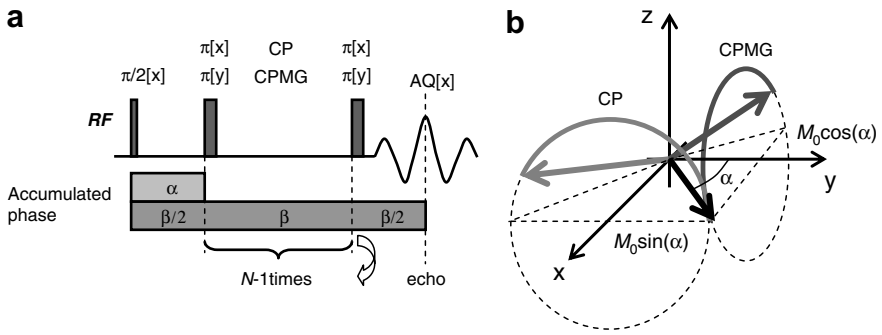

Fig. 1. CP and CPMG pulse sequences (a) with a diagram of the accumulated phase and corresponding magnetization trajectories (b) for on-resonance spins ($\beta = 0$) and with non-zero initial phase α. Note that the magnetization trajectory differs for the CP and CPMG pulse sequence. The CP sequence has a well-determined x magnetization component but an unclear y magnetization component due to imperfections in the refocusing pulse flip angle while in the CPMG sequence the stable and unstable magnetization components are reversed.

inter-echo time. Due to auxiliary phase encoding or other frequency shifting events the magnetization may accumulate an additional initial phase shift α between the excitation pulse and the first refocusing pulse. The phase shift α is the main reason why the conventional CPMG sequence becomes unstable.

A simple illustration of the sequence stability problem is depicted in Fig. 1b, in which the trajectory is plotted for $\beta = 0$. Magnetization that immediately follows the excitation pulse oriented along the y-axis rotates in time between the excitation pulse and the first refocusing pulse by an angle α around the z-axis. Then the magnetization is after N refocusing pulses of flip angle θ rotated by an angle $N\theta$ around the x-axis when the phases of the refocusing pulses correspond to the CP sequence, and is rotated by the same angle around the y-axis when the phases of the refocusing pulses correspond to the CPMG sequence. Note that for the CP sequence the x magnetization component is θ-independent and the y magnetization component is θ-dependent, while for the CPMG sequence the opposite is true (Fig. 1b). In either case the phase of the final magnetization depends on the refocusing pulse flip angle θ and is therefore in general different than the initial phase α. An exception is the case when flip angles of refocusing pulses are ideal, i.e., $\theta = 180°$. Only then is the phase of the final transverse magnetization identical to the phase of the initial transverse magnetization. This problem of phase instability can be overcome if the signals of the θ-dependent magnetization components are suppressed and the remaining signals of the θ-independent magnetization components of both sequences, i.e., $M_0\sin(\alpha)$ of the CP sequence and $M_0\cos(\alpha)$ of CPMG sequence, are summed. A signal obtained in this manner has a phase identical to the initial magnetization phase.

In reality, off-resonance frequencies and so also off-resonance angles β are distributed within the sample. This is especially true for imaging MSE sequences where imaging gradients may induce a large spread of off-resonance angles β (for at least one full angle) within each image voxel. The magnetization of one such component in the Nth echo can be calculated by multiplying matrix rotations [23] that correspond to: the initial magnetization rotation due to auxiliary phase encoding $R_z(\alpha)$, the rotation between the refocusing pulse and the echo (or vice versa) $R_z(\beta/2)$, the rotation due to excitation $R_x(\theta/2)$ and the rotation due to refocusing pulses $R_x(\theta)$, $R_y(\theta)$. This yields the following magnetization vector after the CP and the CPMG sequence

$$\begin{aligned}\vec{M}_{CP}(\alpha,\beta,\theta) &= [R_z(\beta/2)R_x(\theta)R_z(\beta/2)]^N R_z(\alpha)R_x(\theta/2)\vec{M}_0\\ \vec{M}_{CPMG}(\alpha,\beta,\theta) &= [R_z(\beta/2)R_y(\theta)R_z(\beta/2)]^N R_z(\alpha)R_x(\theta/2)\vec{M}_0.\end{aligned} \tag{1}$$

Here the matrix indices denote the axis of rotation. The signal arising from a voxel is then proportional to the average transverse magnetization within the voxel, i.e., to the sum of all magnetization components of different off-resonance angles β divided by the distribution interval. Assuming that the magnetization components are uniformly distributed within the interval from $-\pi$ to π the average transverse magnetization is given by

$$(\overline{M}_x,\overline{M}_y)(\alpha,\theta) = \frac{1}{2\pi}\int_{-\pi}^{\pi}(M_x,M_y)(\alpha,\beta,\theta)\mathrm{d}\beta. \tag{2}$$

The average transverse magnetization in Eq. (2) can then be used to calculate the transverse magnetization magnitude $\overline{M}_{xy} = \sqrt{\overline{M}_x^2 + \overline{M}_y^2}$ and its phase $\bar{\varphi}$, which is for convenience defined as the angle between the transverse magnetization and the y-axis $\bar{\varphi} = \arctan(\overline{M}_x/\overline{M}_y)$. First, Eq. (2) is applied to calculate the average transverse magnetization for the CP and the CPMG sequence. Then these two results are summed to obtain the average magnetization of the two-shot (CP + CPMG) experiment in which signals of the CP and CPMG sequences are summed. The received signal S, which is proportional to the average transverse magnetization, may be defined at the zero receiver phase ($\delta = 0$) as a complex quantity that yields positive real signal when the magnetization is oriented along the $+y$-axis and yields positive imaginary signal when the magnetization is oriented along the $+x$-axis

$$S \equiv \mathrm{i}\overline{M}_x + \overline{M}_y = \overline{M}_{xy}\exp(\mathrm{i}\bar{\varphi}). \tag{3}$$

However, the receiver phase may be non-zero and then the phase of the received signal is shifted for δ so that $S = \overline{M}_{xy} \exp(\mathrm{i}(\bar{\varphi} + \delta))$.

3. Materials and methods

Eqs. (1) and (2) were solved numerically to obtain the average transverse magnetization in the $N = 64$th echo and so the expected signal of the CP, CPMG and CP + CPMG sequence. The correctness of these simulations was then verified by an imaging experiment in which the distribution of electric current density was measured by an MSE imaging sequence in a test sample. The test sample (Fig. 2a) was made of two concentric plastic cylinders. The inner cylinder was 13 mm long and 4 mm in diameter, while the outer cylinder was 10 mm in diameter. Both cylinders were filled with 2% saline. The inner cylinder was capped with electrodes at both ends and was connected to a voltage amplifier capable of delivering 10 V electric pulses of positive or negative polarity. Voltage pulses generated an electric current of 37 mA through the inner cylinder in the axial direction. The amplifier was controlled by TTL pulses from the spectrometer so that the electric pulses could be synchronized with the imaging sequence. The sample was inserted in the MRI magnet with the cylinder axis, i.e., the direction of electric currents, perpendicular to the static magnetic field. Experiments were performed using a 2.35 T horizontal bore Oxford superconducting magnet equipped with Bruker accessories for MR microscopy and a TecMag spectrometer. MR images were processed by a TecMag NT NMR and ImageJ (National Institute of Health, USA) image processing software.

The imaging sequence (Fig. 2b) consisted of an electric current density encoding part (first part) and an acquisition part (second part). The electric current density encoding part consisted of the conventional spin-echo sequence to which two electric voltage pulses of opposite polarity were added: $\pi/2[x] - t_c/2 - \pi[y] - t_c/2$. The electric pulses altered the magnetization phase by an initial phase shift angle α which was proportional to the time integral of the magnetic field change B_c (caused by the electric current) in the direction of the static magnetic field for both electric pulses: $\alpha = \gamma B_c t_c$, where γ is the proton gyromagnetic ratio and t_c is the total duration of both electric pulses. The phase shift of the first electric pulse was reversed by the refocusing pulse and was thus added constructively to the phase shift of the second electric pulse that had the opposite polarity. The imaging part of the sequence consisted of the conventional single-shot RARE imaging sequence with 64 echoes in which the k-space signal from all 64 lines of the image were acquired using standard spin warp phase encode ordering. The imaging sequence was executed twice: once with the phase of all refocusing pulses equal to the phase of the excitation pulse $\pi/2[x] - t_c/2 - \pi[y] - t_c/2 - t_{AQ}/2 - (\pi[x] - AQ)^N$ (as in the standard CP sequence) and once with the phase of all refocusing pulses shifted by 90° with respect to the phase of the excitation pulse $\pi/2[x] - t_c/2 - \pi[y] - t_c/2 - t_{AQ}/2 - (\pi[y] - AQ)^N$ (as in the standard CPMG sequence). The time interval between the two experiments was 10 s. The imaging parameters were: field of view 15 mm, slice thickness 4 mm, imaging matrix 64 by 64, inter-echo delay 2.64 ms and duration of electric voltage pulses 10 ms (each). The imaging slice was oriented perpendicularly to the cylinder axis of the

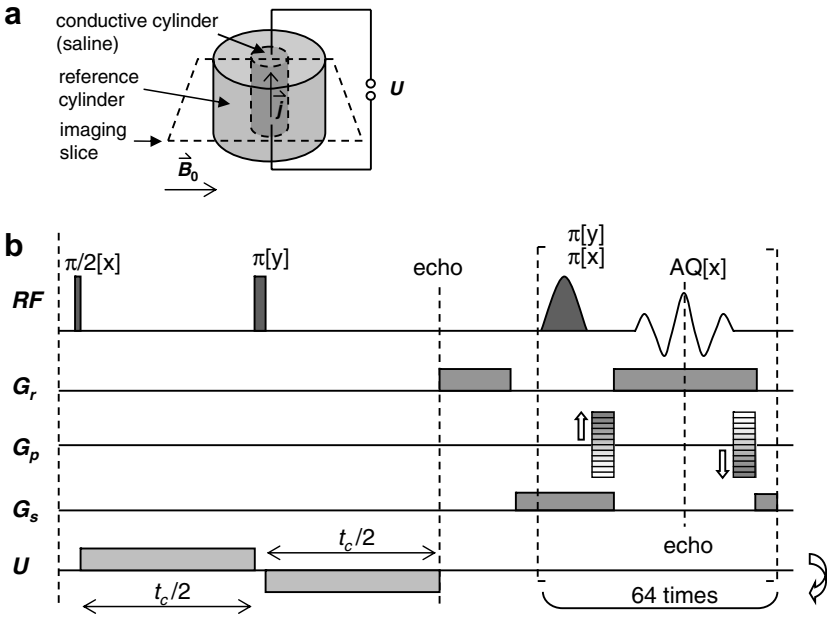

Fig. 2. Arrangement of the cylindrical sample for CD imaging experiment (a) and the two-shot RARE imaging sequence for CDI (b). The sequence consists of an electric current density encoding part (first part) with two electric voltage pulses of opposite polarity, one before and one after the refocusing pulse, and an image encoding part (second part) based on the single-shot RARE imaging sequence with $N = 64$ echoes.

sample. Images of both experiments were summed, thus obtaining, according to the expected theoretical results, the final image (map) with a phase (α) proportional to the static magnetic field change.

The map of the static magnetic field change was then used to calculate the electric current density image as described in [17,18]. Briefly, maps of magnetic field change B_c are used to calculate the current density using Ampere's law $j = 1/\mu_0 \nabla \times B_c$. To calculate one current density component two components of magnetic field change must be known. For example to calculate j_x, B_{c_y} and B_{c_z} must be known: $j_x = 1/\mu_0(\partial B_{c\_z}/\partial y - \partial B_{c\_y}/\partial z)$. The map of B_{c_z} can be measured without sample rotation as z is the direction of the static field and B_{c_z} will directly contribute to the static field change and so to the magnetization phase change. For the other two components this is not the case and if one wants to measure, for example, B_{c_y} the sample must be rotated by 90° so that the previous y-axis becomes parallel to the direction of the static field (former z-axis). Due to the cylindrical symmetry of the sample there was no need to rotate it as the B_{c_y} was obtained simply by rotating the B_{c_z} map by 90°.

According to Ampere's law, the magnetic field increases linearly with the radius of the inner cylinder through which the electric current is flowing, and decreases as one over radius in the outer cylinder where no electric current is flowing. The direction of the magnetic field B_c is perpendicular to the radial and axial direction, so the component of B_c in the direction of the static magnetic field is given by the equation

$$B_c(r,\varphi) = \frac{\mu_0 I}{2\pi R^2} * \begin{cases} r\sin(\varphi) & r \leqslant R \\ (R^2/r)\sin(\varphi) & r > R, \end{cases} \quad (4)$$

where I is the electric current through the inner cylinder, (r,ϕ) is a polar coordinate of a given point in the image, r is the radial distance from the cylinder centre, ϕ is the polar angle with $\phi = 0$ corresponding to the horizontal (x-axis direction), and R is the radius of the inner cylinder. According to the above equation, curves of constant initial phase, i.e., curves of constant magnetic field change, are horizontal lines within the inner cylinder ($y = \text{const.}$), while in the outer cylinder they become circles tangential to the x-axis ($y/r^2 = \text{const.}$).

4. Results and discussion

The average transverse magnetization amplitude $\overline{M}_{xy}$ and its phase $\bar{\varphi}$ as a function of the initial magnetization phase α for various refocusing flip angles θ is depicted in Fig. 3. Graphs in Fig. 3 are simulated at parameters $N = 64$ for the CP, the CPMG and the CP + CPMG sequence. As expected, the amplitude and the phase are error-free for any initial magnetization phase in all three pulse sequences only when the refocusing flip angle is ideal ($\theta = 180°$). In the CP and the CPMG sequence the magnetization amplitude as a function of the initial magnetization phase becomes, for refocusing flip angles other than 180°, sine-modulated due to the loss of the off-phase magnetization component: the y magnetization component in the case of the CP sequence and the x magnetization component in the case of the CPMG sequence. The loss of the off-phase component can also be seen in graphs of the final magnetization phase which get a step-like shape due to dominating 90° and 270° phase in the CP sequence and dominating 0° and 180° phase in the CPMG sequence. This is unlike the result for the CP + CPMG sequence, which is obtained by summation of the average transverse magnetizations of the CP and the CPMG sequences. In this case the magnetization amplitude is independent of the initial magnetization phase; however, it is still dependent on the refocusing pulse flip angle. Most importantly, the final phase of the transverse magnetization is identical to the initial phase for any refocusing pulse flip angle. This result agrees well with Eq. (2) which predicts such behavior. Irregularities in $\overline{M}_{xy}$ graphs, i.e., asymmetry in dips for the CP and the CPMG sequence and oscillations for the CP + CPMG sequence, are due to imperfect excitation pulse flip angles at θ other than 180°.

Results of the RARE based CDI sequences (Fig. 2b) which were used for experimental verification of the presented theory are shown in Fig. 4. The CPMG imaging sequence produces nice results when electric current pulses are off so there is no initial phase variation and $\alpha = 0°$ everywhere in the sample (magnitude image in Fig. 4a). Uniformity of the initial phase can be seen in the phase image of the test sample (Fig. 4i, phase in the range 0°–360° is proportional to image brightness) as well as in the real signal component image of the test sample (Fig. 4e) in which the intensity is proportional to $\Re(S) = M_0\cos(\alpha + \delta)$, where δ is the phase difference between the transmitter phase and the received signal phase. Ideally $\delta = 0$, but in the presented experiment it was equal to $\delta = 190°$. The non-zero phase δ does not introduce any artefacts in the image, it just shifts its phase from α to $\alpha + \delta$. In CDI and many other methods the final image is obtained after subtraction of phase maps of different auxiliary encodings so that the phase shift δ is cancelled during subtraction and has no influence on the final result. The absence of electric current is also visible in the calculated electric current density image in Fig. 4m in which the electric current density in a range from -3500 A/m^2 to 3500 A/m^2 is depicted by image brightness. In the image both cylinders, the outer reference cylinder with no electric current and the inner one which was connected to the electrodes, have identical image brightness, which indicates that no electric current was flowing through the inner cylinder.

A pattern of dark and bright bands whose distribution corresponds to the above description of curves of constant initial phase is seen not only in the real signal component images (Fig. 4f–h) where one would expect such a pattern, but also in the magnitude images in Fig. 4b and c. This surprising result agrees with our theory, which predicts refocusing of the initial x magnetization component ($\alpha = 90°$,

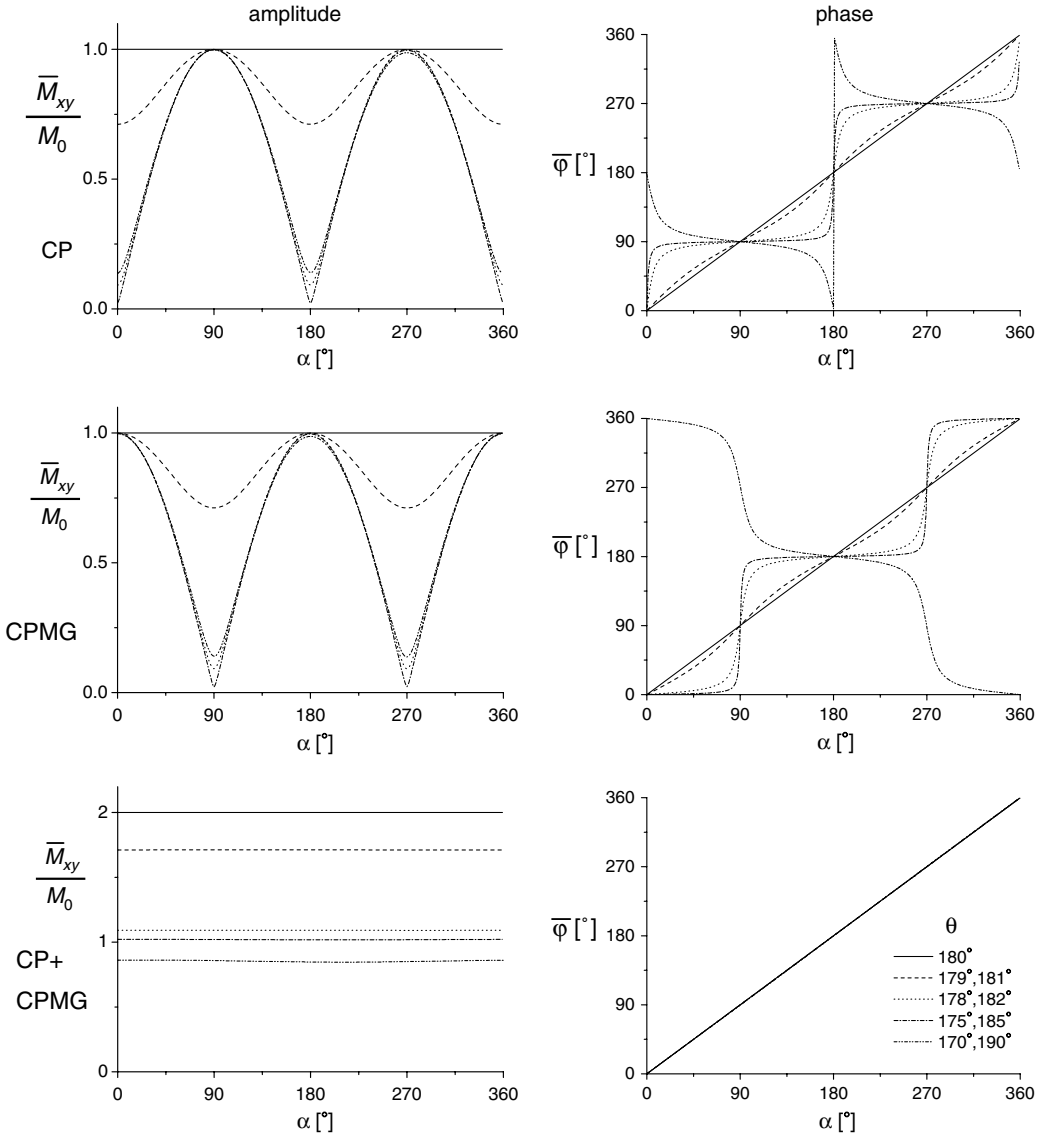

Fig. 3. Computer simulations of the average transverse magnetization magnitude $\overline{M}_{xy}$ (left column) and phase $\bar{\varphi}$ (right column) in the $N = 64$th echo of the CP, the CPMG and the CP + CPMG sequence as a function of the initial magnetization phase α for refocusing pulses of various flip angles θ.

270°, ...) for the CP sequence and refocusing of the initial y magnetization component ($\alpha = 0°, 180°, \ldots$) for the CPMG sequence. Transverse magnetization for other initial phases is not refocused and appears dark in magnitude images. A consequence of imperfect refocusing is also seen in phase images in Fig. 4j (CP sequence) and k (CPMG sequence) where in each case the phase has just two different values corresponding to $\alpha = 90°$, 270° for the CP sequence and $\alpha = 0°$, 180° for the CPMG sequence. Real signal component images in Fig. 4f and g should be identical but they are not due to imperfect refocusing. Due to large errors in the acquisition of the initial phase the images cannot be used for calculating the electric current density or in principle any similar event that may change the initial phase of magnetization. Calculated electric current density images in Fig. 4n (CP sequence) and Fig. 4o (CPMG sequence) are grossly distorted and provide entirely incorrect information on the direction and the magnitude of the electric current density.

The way to avoid this problem of sequence instability with respect to the initial phase is, according to the theory presented previously, to sum the signals of the MSE sequences acquired with the CP and CPMG phase schemes, in this case to sum their corresponding images. The magnitude image obtained by such a two-shot RARE CDI sequence is presented in Fig. 4d. As expected, the magnitude image in Fig. 4d does not have any errors in the form of dark and bright bands that are present in magnitude images acquired with the one phase scheme (the CP phase scheme in Fig. 4b and the CPMG phase scheme in Fig. 4c). As the presence of these bands is a sign of imperfect refocusing it may be concluded that the summation of images acquired with CP and CPMG sequences yields an image where magnetization components for all initial phases α

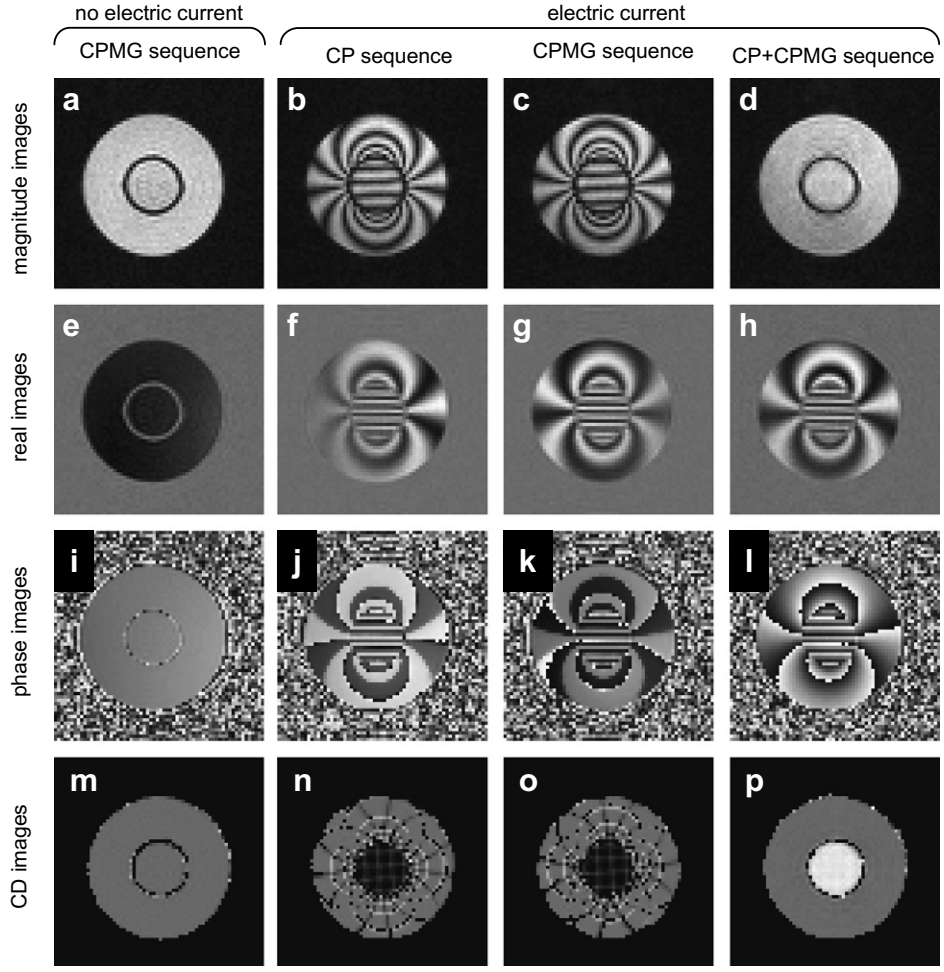

Fig. 4. Images of the saline-containing test sample that consisted of two concentric cylinders: the inner one with or without electric current in the axial direction and the outer one with no electric current used as a reference. Images were acquired by the single-shot RARE based CDI sequences from Fig. 2b. When no electric current was flowing the initial phase was zero and the magnetization was perfectly refocused by the CPMG sequence so the magnitude (a) and the real signal component (e) images have no artefacts. Uniformity of the initial phase is clear in the phase image (i) in which the initial phase shifted by an offset of 190° is shown in the range from 0° (black) to 360° (white). The electric current density image (m), which shows electric current densities from -3500 A/m^2 (black) to 3500 A/m^2 (white) distinctly shows no current. Note that the black background had no current but was set to black for clarity. When electric currents were on, the initial phase was no longer zero but it became proportional to the electric current magnetic field change and was thus continuously varying across the sample. Due to the inability of the CP (b) and CPMG (c) sequences to refocus magnetization components for all different initial phases the magnitude images have signal voids in the form of dark bands. The magnitude image obtained by summing the signals of the CP and CPMG sequences (d) has no signal voids even though the initial phase was non-zero, which can be seen in the corresponding real signal component image (h) and the phase image (l). The latter has a phase which changes continuously from 0° to 360° which is not the case for phase images of CP (j) and CPMG (k) sequences in which the phase has just two discrete values. Due to imperfect magnetization refocusing, calculated CDI images of CP (n) and CPMG (o) sequences are highly distorted while the CDI image of the summed CP and CPMG experiments (p) is free from artefacts and clearly shows electric current through the inner cylinder of 3000 A/m^2.

are equally well refocused. This is also seen in the real signal component image in Fig. 4h where the pattern of bright and dark bands is fully consistent with previous results obtained by the conventional CDI methods on the same test sample [18], as well as in the phase image in Fig. 4l where the phase changes continuously from 0° to 360° and does not have just two discrete values as in images in Fig. 4j and k. The soundness of this result is also apparent in the calculated electric current density image in Fig. 4p which is flawless in the sense of artefact-free CD distribution. The image shows a distinct difference between no electric current in the reference cylinder which is gray (ROI-based calculation yielded current density of -20 ± 100 A/m^2) and the inner cylinder with an electric current of 3060 ± 100 A/m^2 which is bright (the image background with no current, which should have the same gray level as the reference cylinder, was set to black for better perception of the sample). This result agrees well with a direct current density calculation, i.e., current divided by the inner cylinder cross-section area, which yields current density of 2940 A/m^2.

Just one run of the proposed two-shot RARE based CDI method is for a general geometry sample not enough. The CD image could be calculated from data acquired in

just one sample orientation due to the cylindrical symmetry of the sample and therefore cylindrical symmetry of the electric current density distribution within it. In general, for 2D CDI of asymmetrical samples, the sample must be rotated by 90° around the axis parallel to the direction of applied electric currents so that the remaining component of the induced magnetic field is acquired in a second run of the two-shot CDI method. For 3D CDI, acquisition in three perpendicular orientations is needed to map three different components of the induced magnetic field. This implies running the two-shot CDI method three times.

Fast electric current density imaging is not the only possible application of the two-shot RARE CDI sequence. Auxiliary phase encoding in the preparation part of the sequence can be modified so that it becomes sensitive to other physical phenomena instead of electric currents. For example, by replacing electric voltage pulses with a pair of magnetic field gradient pulses the sequence will become sensitive to any displacement of the sample. This may be due to flow or deformation that occurs during the application of a bipolar gradient pair. The preparation part of the sequence without any gradient or electric pulses where the refocusing pulse is shifted from its centre is sensitive to precession frequency shifts and can thus be used for measuring susceptibility effects, chemical shifts, or other events that may change the precession frequency such as the sample temperature or its pH. Problems with the MSE sequence instability may also be encountered if for some reason the delay between the excitation pulse is not exactly equal to one half of the delay between the refocusing pulses in the MSE pulse train. Different spins then get different initial phases and those with the non-MG component will not get refocused in the standard MSE pulse train. This problem can be eliminated with the two-shot RARE method, i.e., by summing signals of the CP and CPMG imaging sequences. Of course there are other solutions to this problem, as discussed in the introduction: use of dephasing gradients [9], incoherent U-FLARE method [8] or application of refocusing pulses with quadratic phases [11], but they either destroy half of the transverse magnetization or they are quite complicated to perform. The method we propose is simple and quite robust. Two single-shot RARE experiments with refocusing pulses of different phase are more time-consuming than a single experiment. Single-shot methods lose half of the transverse magnetization (except for the Le Roux [11] method), so to obtain identical SNR as in the proposed two-shot RARE method two signal averages are needed, resulting in the same time consumed. However, SNR in the two-shot RARE method may be further improved by the factor of $\sqrt{2}$ if the signal and so the noise of the non-MG magnetization component is zeroed before the summation. To discriminate between the MG and the non-MG components of the signal accurately a spatial map of the receiver phase δ is required. With this improvement, the SNR ratios between Le Roux's method, the two-shot RARE method with the non-MG signal zeroed, and the conventional single-shot methods [8–10] are after two successive signal acquisitions equal to $\sqrt{2}:1:1/\sqrt{2}$.

In the single-shot RARE method, a signal for the whole 2D image is acquired after just one signal excitation. In principle the presented theory applies also to other spin-echo modalities like standard RARE or 3D-RARE imaging that are not single-shot imaging methods. It is also important that the time interval between individual CP and CPMG experiments is large enough so that the magnetization fully relaxes and the CP and CPMG experiment start with identical initial conditions. Otherwise the residual magnetization of the previous experiment may interfere with the magnetization amplitude and phase in the current experiment. In addition, the receiver phase as well as all sample related conditions must remain unchanged between the two experiments. This may preclude the use of the method in diffusion weighted imaging where even slightest sample movement may result in large differences in the initial phase shifts between the experiments.

An alternative that would enable auxiliary phase encoding in a single-shot acquisition would be to use the echo-planar method (EPI) [24]. In EPI problems associated with the instability at certain initial phases of transverse magnetization would not arise. However, EPI is very sensitive to any off-resonance frequencies and susceptibility effects [25] and is therefore less robust than the proposed two-shot RARE method. The presented two-shot RARE method is also a very useful extension to the conventional CDI method for all cases where the imaging speed or low number of delivered electric pulses are of a high priority.

5. Conclusion

MSE sequences are very sensitive to the initial phase of transverse magnetization. The initial phase may be shifted in the time interval after the excitation pulse and before the start of the MSE pulse train by an auxiliary encoding or by events such as diffusion weighting, eddy currents, patient movement or susceptibility effects. The CPMG sequence, which is proven to be very effective when the initial phase is uniform and equal to zero so that the initial magnetization is oriented along the y-axis or $-y$-axis (assuming the excitation pulse rotates the magnetization around the x-axis), fails for other initial phases. The same is true for the CP sequence, except that it is stable for the initial magnetization oriented along the x-axis or $-x$-axis. So, neither of the two MSE sequences is stable for an arbitrary initial phase of the transverse magnetization. In this paper, we have proven first theoretically and then experimentally by an electric current density experiment combined with the single-shot RARE imaging method, that the sum of the CP and CPMG imaging sequences produces a stable scheme that refocuses any initial transverse magnetization regardless of its phase. The proposed two-shot RARE method preserves the initial phase of transverse magnetization and can therefore register the phase accumulated by auxiliary phase encoding in the preparation part of the

sequence correctly. This method is quite versatile as many different physical phenomena may be observed by designing corresponding preparation sequences via phase shifts of the initial transverse magnetization.

Acknowledgment

The author thanks Andrej Pintar for proofreading the manuscript.

References

[1] H.Y. Carr, E.M. Purcell, Effects of diffusion on free precession in nuclear magnetic resonance experiments, Phys. Rev. 94 (1954) 630–638.
[2] S. Meiboom, D. Gill, Modified spin-echo method for measuring nuclear relaxation times, Rev. Sci. Instr. 29 (1958) 688–691.
[3] J. Hennig, A. Nauerth, H. Friedburg, RARE imaging: a fast imaging method for clinical MR, Magn. Reson. Med. 3 (1986) 823–833.
[4] A.A. Maudsley, Modified Carr–Purcell–Meiboom–Gill sequence for NMR Fourier imaging applications, J. Magn. Reson. 69 (1986) 488–491.
[5] T. Gullion, D.B. Baker, M.S. Conradi, New, compensated Carr–Purcell sequences, J. Magn. Reson. 89 (1990) 479–484.
[6] J. Hennig, Multiecho imaging sequences with low refocusing flip angles, J. Magn. Reson. 78 (1988) 397–407.
[7] D.G. Norris, Ultrafast low-angle RARE: U-FLARE, Magn. Reson. Med. 17 (1991) 539–542.
[8] D.G. Norris, P. Bornert, T. Reese, D. Leibfritz, On the application of ultra-fast RARE experiments, Magn. Reson. Med. 27 (1992) 142–164.
[9] D.C. Alsop, Phase insensitive preparation of single-shot RARE: application to diffusion imaging in humans, Magn. Reson. Med. 38 (1997) 527–533.
[10] F. Schick, SPLICE: sub-second diffusion-sensitive MR imaging using a modified fast spin-echo acquisition mode, Magn. Reson. Med. 38 (1997) 638–644.
[11] P. Le Roux, Non-CPMG fast spin echo with full signal, J. Magn. Reson. 155 (2002) 278–292.
[12] J.B. Murdoch, An "Effective" method for generating spin-echo intensity expression, Proc. 2nd SMR Sci. Meet., San Francisco, CA, 1994, p. 1145.
[13] M.W. Vogel, P.M. Pattynama, F.L. Lethimonnier, P. Le Roux, Use of fast spin echo for phase shift magnetic resonance thermometry, J. Magn. Reson. Imaging 18 (2003) 507–512.
[14] P. Le Roux, Simplified model and stabilization of SSFP sequences, J. Magn. Reson. 163 (2003) 23–37.
[15] K.A. Il'yasov, J. Hennig, Single-shot diffusion-weighted RARE sequence: application for temperature monitoring during hyperthermia session, J. Magn. Reson. Imaging 8 (1998) 1296–1305.
[16] R.V. Mulkern, P.S. Melki, P. Jakab, N. Higuchi, F.A. Jolesz, Phase-encode order and its effect on contrast and artifact in single-shot RARE sequences, Med. Phys. 18 (1991) 1032–1037.
[17] M. Joy, G. Scott, M. Henkelman, In vivo detection of applied electric currents by magnetic resonance imaging, Magn. Reson. Imaging 7 (1989) 89–94.
[18] I. Sersa, O. Jarh, F. Demsar, Magentic resonance microscopy of electric currents, J. Magn. Reson. A111 (1994) 93–99.
[19] U. Mikac, A. Demsar, F. Demsar, I. Sersa, A study of tablet dissolution by magnetic resonance electric current density imaging, J. Magn. Reson. (2006).
[20] E. Kossel, M. Weber, R. Kimmich, Visualization of transport: NMR microscopy experiments with model objects for porous media with pore sizes down to 50 micron, Solid State Nucl. Magn. Reson. 25 (2004) 28–34.
[21] G.C. Scott, M.L. Joy, R.L. Armstrong, R.M. Henkelman, RF current density imaging in homogeneous media, Magn. Reson. Med. 28 (1992) 186–201.
[22] S.A. Solazzo, Z. Liu, S.M. Lobo, M. Ahmed, A.U. Hines-Peralta, R.E. Lenkinski, S.N. Goldberg, Radiofrequency ablation: importance of background tissue electrical conductivity—an agar phantom and computer modeling study, Radiology 236 (2005) 495–502.
[23] I. Sersa, S. Macura, Excitation of arbitrary shapes by gradient optimized random walk in discrete *k*-space, Magn. Reson. Med. 37 (1997) 920–931.
[24] P. Mansfield, Multi-planar image formation using NMR spin echoes, J. Phys. C 10 (1977) L55–L58.
[25] F. Farzaneh, S.J. Riederer, N.J. Pelc, Analysis of T2 limitations and off-resonance effects on spatial resolution and artifacts in echo-planar imaging, Magn. Reson. Med. 14 (1990) 123–139.